# Accessing transverse nucleon and gluon distributions in heavy nuclei using coherent vector meson photoproduction at high energies in ion ultraperipheral collisions

V. Guzey, M. Strikman, and M. Zhalov

Phys. Rev. C **95**, 025204 — Published 13 February 2017

DOI: 10.1103/PhysRevC.95.025204

# Accessing transverse nucleon and gluon distributions in heavy nuclei using coherent vector meson photoproduction at high energies in ion ultraperipheral collisions

V. Guzey,[1] M. Strikman,[2] and M. Zhalov[1]

[1] *National Research Center "Kurchatov Institute", Petersburg Nuclear Physics Institute (PNPI), Gatchina, 188300, Russia*

[2] *Department of Physics, The Pennsylvania State University, State College, PA 16802, USA*

Using the theoretical approaches describing well the available data on $t$-integrated coherent photoproduction of light and heavy vector mesons in Pb-Pb UPCs at the LHC in Run 1, we calculate the momentum transfer distributions for this process for $\rho$ and $J/\psi$ vector mesons in the kinematics of Run 2 at the LHC. We demonstrate that nuclear shadowing not only suppresses the absolute value of the cross sections, but also shifts the momentum transfer distributions toward smaller values of the momentum transfer $|t|$. This result can be interpreted as a broadening in the impact parameter space of the effective nucleon density in nuclei by 14% in the case of $\rho$ and the nuclear gluon distribution by $5-11\%$ in the case of $J/\psi$.

## I. INTRODUCTION

High-energy exclusive (elastic) processes with various beams and targets provide information on the distribution of scattering centers in the target in the plane perpendicular to the beam direction (the impact parameter plane), which makes possible the transverse imaging of the target. Its examples are well-known and numerous. Measuring the intermediate energy elastic scattering of electrons and protons on nuclei allows one to reconstruct the charge and matter (proton+neutron) distributions in nuclei, respectively. The data on elastic proton–proton scattering at high energies are widely used to learn about the proton profile in the impact parameter space. The recent relativistic analyses of elastic form factors of hadrons (proton, neutron, pion) measured in elastic scattering were carried out in terms of the transverse quark densities. More generally, generalized parton distribution functions (GPDs) accessed in hard exclusive processes encode information of the quark and gluon distributions in a given target (including transitions between the hadronic states) in terms of light-cone momentum fractions and the impact parameter. Thus, they at least in principle hold the promise for obtaining a three-dimensional picture of hadrons and nucleus in Quantum Chromodynamics (QCD), which is one of the key objectives of the physics program of a future Electron-Ion Collider [1].

Part of this program involving high energy quasireal photons overlaps with studies of proton–proton, proton–nucleus and nucleus–nucleus ultraperipheral collisions (UPCs) [2] at the Large Hadron Collider (LHC). In particular, during Run 1 in Pb-Pb UPCs, the ALICE collaboration [3] measured coherent photoproduction of $\rho$ mesons on heavy nuclei and the ALICE [4, 5] and CMS [6] collaborations measured coherent $J/\psi$ photoproduction on nuclei. Comparison of these data with numerous model calculations [7–14] demonstrated that the best agreement is observed only if the calculations account for the effect of strong nuclear shadowing, which suppresses the $\rho$ photoproduction cross section by approximately a factor of six and the $J/\psi$ cross section by approximately a factor of three. In particular, it was shown that the Gribov–Glauber approach to nuclear shadowing combined with phenomenology of real and virtual photon diffraction [8, 11] provides a good description of the data. While the statistics of $\rho$ and $J/\psi$ photoproduction in Run I was insufficient for the detailed study of the transverse momentum distributions of vector mesons in these processes, some hints of such shifting have been observed by both ALICE [3] and STAR [15, 16] collaborations. Note that the preliminary PHENIX data on coherent and incoherent $J/\psi$ photoproduction in Au-Au UPCs at $\sqrt{s_{NN}} = 200$ GeV accompanied by forward neutron emission [17] probes the nuclear gluon distribution at the momentum fraction $x \approx 0.015$, where the nuclear shadowing suppression is not large; see the good description of this data in Ref. [18]. At the same time, the limited precision of the data and its wide binning in $t$ along with the expected small gluon nuclear shadowing make it very difficult to study the modification of the $t$ distribution discussed in this work. The much higher statistics of Run 2 at the LHC allows one to study the influence of strong nuclear shadowing on the transverse momentum distributions.

In this paper, using the theoretical approaches describing well the available data from Run 1, we extend our previous study [19] and calculate the momentum transfer distributions for coherent photoproduction of $\rho$ and $J/\psi$ vector mesons on nuclei in Pb-Pb UPCs in Run 2 at the LHC. We show that nuclear shadowing not only suppresses the absolute value of the cross sections, but also changes the shape of the differential cross sections by shifting the momentum transfer distributions toward smaller values of the momentum transfer $|t|$. One can interpret these results as an effective broadening in the impact parameter space of the nucleon density in nuclei in the case of $\rho$ and the nuclear gluon distribution in the case of $J/\psi$. It is a generic and model-independent consequence of the fact that nuclear shadowing suppression at small impact parameters is stronger than that at the nucleus periphery.

## II. COHERENT PHOTOPRODUCTION OF LIGHT AND HEAVY VECTOR MESONS ON NUCLEI

Collisions of ions at large impact parameters, which are called ultraperipheral collisions (UPCs) in the literature, give an opportunity to study photon-initiated processes at unprecedentedly high energies [2]. The cross section of coherent vector meson $V$ photoproduction in nucleus–nucleus UPCs reads:

$$\frac{d\sigma_{AA\to VAA}(y)}{dydt} = N_{\gamma/A}(y)\frac{d\sigma_{\gamma A\to VA}(y)}{dt} + N_{\gamma/A}(-y)\frac{d\sigma_{\gamma A\to VA}(-y)}{dt}\,, \tag{1}$$

where $N_{\gamma/A}$ is the flux of equivalent photons emitted by either of the nuclei; $d\sigma_{\gamma A\to VA}(y)/dt$ is the differential cross section of coherent vector meson photoproduction on nuclei; $y$ is the vector meson rapidity and $t$ is the invariant momentum transfer squared. For a given $y$, the photon has the energy of $\omega = (M_V/2)e^{y}$, when emitted by the nucleus moving in the direction of $V$, or the energy of $\omega = (M_V/2)e^{-y}$, when emitted by the nucleus moving in the opposite direction. Note that allowing the final nucleus to disintegrate in the $\gamma A \to VA'$ process, one can use Eq. (1) to calculate also incoherent vector meson photoproduction on nuclei in UPCs.

In the $\rho$ meson case, the coherent $\gamma A \to \rho A$ cross section in the approach based on the combination of the vector meson dominance (VMD) model and the Glauber model of nuclear shadowing (we collectively called it VMD-GM) reads [20]:

$$\frac{d\sigma^{\rm VMD-GM}_{\gamma A\to\rho A}(W_{\gamma p})}{dt} = \left(\frac{e}{f_\rho}\right)^2 \frac{(1+\eta^2)\sigma^2_{\rho N}}{16\pi}\left|\int d^2\vec{b}\, e^{i\vec{q}_\perp\vec{b}}\int dz\rho_A(b,z)e^{iq_\parallel z}e^{-\frac{1}{2}(1-i\eta)\sigma_{\rho N}\int_z^\infty dz'\rho_A(b,z')}\right|^2 . \tag{2}$$

In Eq. (2), $W_{\gamma p}$ is the invariant photon–nucleus energy per nucleon; $\sigma_{\rho N}$ is the total vector meson–nucleon cross section; $f_\rho$ is the $\gamma-\rho$ coupling constant; $\eta$ is the ratio of the real to the imaginary parts of the $\gamma p\to\rho p$ amplitude; $\rho_A(b,z)$ is the nucleon density, which depends on the longitudinal ($z$) and transverse ($\vec{b}$) coordinates of the active nucleon in a nucleus; $\vec{q}_\perp$ and $q_\parallel$ are the transverse and longitudinal components of the momentum transfer, $t=-q_\parallel^2-\vec{q}_\perp^{\,2}$. This approach and its generalizations [21, 22] taking into account the influence of the higher $\rho'$ component of the photon wave function and nondiagonal $\rho\leftrightarrow\rho'$ transitions provide a good description of the available fixed-target data and the RHIC data on $\rho$ photoproduction in Au-Au UPCs at $\sqrt{s_{NN}}=62.4$ GeV and 130 GeV corresponding to $W_{\gamma p}\le 10$ GeV [23, 24].

With an increase of the photon energy, the inclusion of only lower hadronic components ($\rho'$) of the photon wave function becomes insufficient and one needs to take into account the effect of inelastic (Gribov) nuclear shadowing corresponding to the photon diffraction into large masses. In Ref. [8], this was realized using the Good–Walker formalism of cross section fluctuations [25, 26] by introducing the distribution $P_V(\sigma)$ giving the probability for the photon to interact with a nucleon target with the cross section $\sigma$. Note that in addition to significant inelastic nuclear shadowing, the cross section fluctuations result in the reduction of the effective $\rho$ meson–nucleon cross section probed in the $\gamma p\to\rho p$ process compared to the additive quark model estimate. The resulting approach, which was called the modified VMD–Glauber–Gribov model (mVMD-GGM) in Ref. [8], leads to good description of all available data on coherent $\rho$ photoproduction on nuclei, including the RHIC Au-Au UPC data at $\sqrt{s_{NN}}=200$ GeV [27] and the LHC Pb-Pb UPC data at $\sqrt{s_{NN}}=2.76$ TeV [3] corresponding to $W_{\gamma p}>10$ GeV.

Neglecting the longitudinal momentum transfer, the $\gamma A\to\rho A$ cross section in the mVMD-GGM approach has the following form in the high-energy limit:

$$\frac{d\sigma^{\rm mVMD-GGM}_{\gamma A\to\rho A}(W_{\gamma p})}{dt} = \left(\frac{e}{f_\rho}\right)^2 \frac{1}{4\pi}\left|\int d^2\vec{b}\, e^{i\vec{q}_\perp\vec{b}}\int d\sigma P_V(\sigma)\left(1-e^{-\frac{1}{2}(1-i\eta)\sigma T_A(b)}\right)\right|^2 , \tag{3}$$

where $T_A(b)=\int dz\rho_A(b,z)$ is the density of nucleons in the transverse plane (the nuclear optical density) and $P_V(\sigma)$ is the distribution over cross section fluctuations for the $\gamma N\to\rho N$ transition. This normalized distribution is centered around the effective $\rho$ meson–nucleon cross section extracted from the HERA $\gamma p\to\rho p$ data and has the dispersion determined by the photon diffractive dissociation $\gamma p\to Xp$ into large masses measured at the Fermilab, see details in Ref. [8].

Coherent nuclear scattering at $t\neq 0$ is always accompanied by incoherent and inelastic processes, which contaminate the elastic signal. Hence, in practice one needs to separate the coherent and incoherent signals and examine the smearing of diffractive minima by the incoherent contribution. In UPCs, incoherent processes are characterized by inelastic final states in the forward direction and can be separated from the coherent process by examining the $t$ dependence. To address these issues, we calculate the incoherent $\gamma A\to\rho A'$ cross section ($A'\neq A$ denotes products of nuclear disintegration) using the following well-known expression [20]:

$$\frac{d\sigma^{\rm VMD-GM}_{\gamma A\to\rho A'}(W_{\gamma p})}{dt} = \frac{d\sigma_{\gamma p\to\rho p}(W_{\gamma p})}{dt}\int d^2\vec{b}\, T_A(b)e^{-\sigma^{\rm in}_{\rho N}T_A(b)}\,, \tag{4}$$

where $\sigma_{\rho N}^{\rm in} = \sigma_{\rho N} - \sigma_{\rho N}^2/(16\pi B_\rho)$ is the inelastic $\rho$–nucleon cross section; $B_\rho = 10.9 + 0.46\ln(W_{\gamma p}/72\ {\rm GeV})^2\ {\rm GeV}^{-2}$ is the slope of the $t$ dependence of the $\gamma p \to \rho p$ cross section at the relevant energies [28, 29]. Note that in Eq. (4) we neglected the effect of cross section fluctuations and, thus, obtained the upper limit on the inelastic cross section. The key feature of incoherent photoproduction on nuclear targets is that the $t$ dependence of the nuclear cross section is dictated by the $t$ dependence of photoproduction on the nucleon:

$$\frac{d\sigma_{\gamma p\to\rho p}(W_{\gamma p},t)}{dt} = \left(\frac{e}{f_\rho}\right)^2 \frac{(1+\eta^2)\sigma_{\rho N}^2}{16\pi} e^{B_\rho t}\,. \tag{5}$$

Turning to the $J/\psi$ case, we notice that the main interest in studying exclusive $J/\psi$ photoproduction at high energies is that it gives an almost direct access to the gluon distribution $g_T(x,\mu^2)$ in a given target [30, 31] at the resolution scale of $\mu^2 = \mathcal{O}(m_c^2)$ ($m_c$ is the mass of the charm quark) in the kinematical region, where the gluons carry a small fraction $x = M_{J/\psi}^2/W_{\gamma p}^2 \ll 1$ of the target momentum. To the leading orders in the strong coupling constant and the non-relativistic expansion for the $J/\psi$ distribution amplitude, the cross section of coherent $J/\psi$ photoproduction on nuclei in the high-energy limit is usually written in the following form, see, e.g., Ref. [12]:

$$\frac{d\sigma_{\gamma A\to J/\psi A}}{dt} = \frac{d\sigma_{\gamma p\to J/\psi p}(t=0)}{dt}\left(\frac{R_{g,A}}{R_{g,p}}\right)^2\left(\frac{g_A(x,\mu^2)}{Ag_p(x,\mu^2)}\right)^2 F_A^2(t)\,, \tag{6}$$

where $d\sigma_{\gamma p\to J/\psi p}(t=0)/dt$ is the differential cross section on the proton at $t\approx 0$; $g_A(x,\mu^2)/[Ag_p(x,\mu^2)]$ is the ratio of the nuclear and proton gluon distributions; $F_A(t) = \int d^2b\, e^{i\vec{q}_\perp\vec{b}} T_A(b)$ is the nuclear form factor; $R_{g,A}$ and $R_{g,p}$ are the so-called skewness factors for the nucleus and proton gluon GPDs, respectively, which can be estimated using the small-$x$ behavior of the corresponding gluon distributions [32]. Note that while the leading order description of $J/\psi$ photoproduction is subject to sizable corrections [33, 34], we expect that they largely cancel in Eq. (6).

Equation (6) assumes that nuclear shadowing does not affect the $t$ dependence of $d\sigma_{\gamma A\to J/\psi A}/dt$, which is then given by the nuclear form factor squared $F_A^2(t)$. This is an approximation valid, when the effect of nuclear shadowing is insignificant. However, as we discussed in the Introduction, this is not the case. Hence, strong nuclear shadowing should also modify the $t$ dependence of the $d\sigma_{\gamma A\to J/\psi A}/dt$ cross section. Generalizing Eq. (6) to the case of large nuclear shadowing, we obtain:

$$\frac{d\sigma_{\gamma A\to J/\psi A}}{dt} = \frac{d\sigma_{\gamma p\to J/\psi p}(t=0)}{dt}\left(\frac{R_{g,A}}{R_{g,p}}\right)^2\left(\frac{g_A(x,t,\mu^2)}{Ag_p(x,\mu^2)}\right)^2\,, \tag{7}$$

where $g_A(x,t,\mu^2)$ is the nucleus generalized gluon distribution in the special limit, when both gluon lines carry the equal light-cone momentum fractions of $x$. In this case, GPDs can be expressed in terms of the impact parameter dependent PDFs [35]. In particular, we have for $g_A(x,t,\mu^2)$:

$$g_A(x,t,\mu^2) = \int d^2\vec{b}\, e^{i\vec{q}_\perp\vec{b}} g_A(x,b,\mu^2)\,, \tag{8}$$

where $xg_A(x,b,\mu^2)$ is the impact parameter dependent gluon nuclear PDF [36, 37], which gives the probability to find in a nucleus a gluon with the light-cone momentum fraction $x$ at the transverse distance $b$ from the nucleus (center-of-mass) center. Using the results of Ref. [18] for the calculation of $g_A(x,b,\mu^2)$, the expression for the cross section of coherent $J/\psi$ photoproduction on nuclei reads:

$$\frac{d\sigma_{\gamma A\to J/\psi A}}{dt} = \frac{d\sigma_{\gamma p\to J/\psi p}(t=0)}{dt}\left|\int d^2\vec{b}\, e^{i\vec{q}_\perp\vec{b}}\left[\left(1-\frac{\sigma_2}{\sigma_3}\right)T_A(b) + \frac{2\sigma_2}{\sigma_3^2}\Re e\left(1-e^{-\frac{1}{2}\sigma_3(1-i\eta)T_A(b)}\right)\right]\right|^2\,. \tag{9}$$

Equation (9) is a series in powers of $T_A(b)$ (numbers of interactions with target nucleons), which builds the nuclear shadowing suppression. The term proportional to $T_A^2(b)$ describes the interaction with two nucleons, whose strength is given by the $\sigma_2$ cross section:

$$\sigma_2 = \frac{16\pi B_{\rm diff}}{(1+\eta^2)xg_p(x,\mu^2)}\int_x^{0.1} dx_{I\!P}\,\beta g_p^{D(3)}(\beta, x_{I\!P},\mu^2)\,, \tag{10}$$

where $B_{\rm diff}\approx 6\ {\rm GeV}^{-2}$ is the slope of the $t$ dependence of the cross section of hard inclusive diffraction on the proton in deep inelastic scattering (DIS) $\gamma^* p\to Xp$ [38]; $\eta\approx 0.17$ is the ratio of the real to imaginary parts of the $\gamma^* p\to Xp$ amplitude estimated using the Gribov–Migdal relation; $g_p^{D(3)}(\beta, x_{I\!P},\mu^2)$ is the gluon diffractive parton distribution

of the proton [38, 39], which depends on the diffractive exchange ("Pomeron") momentum fraction $x_{I\!P}$, the gluon momentum fraction $\beta$, and the scale $\mu^2$. Using the leading order (LO) H1 diffractive PDFs and the CTEQ6L1 gluon density [40], we find that $\sigma_2 = 21$ mb at $x = 0.001$ and $\mu^2 = 3$ GeV$^2$. The interaction with three and more nucleons is modeled by the effective cross section of $\sigma_3$, which is constrained using the formalism of cross section fluctuations in Ref. [36]. We estimate that $\sigma_3 = 26-45$ mb, which presents the main source of theoretical uncertainties on $g_A(x, b, \mu^2)$ in this approach. One can see from Eq. (9) that nuclear shadowing (the sum of terms proportional to $T_A^n(b)$, with $n \geq 2$) affects not only the magnitude of $\sigma_{\gamma A\to J/\psi A}$, but also the $t$ dependence of $d\sigma_{\gamma A\to J/\psi A}/dt$.

It is important to note that while Eqs. (6) and (9) give discernibly different predictions for $d\sigma_{\gamma A\to J/\psi A}/dt$, their predictions for the $t$ integrated $\sigma_{\gamma A\to J/\psi A}$ cross section differ by less than approximately 15% (the approximate expression gives the larger cross section than the exact one). This gives a less than 8% correction to the nuclear suppression factor of $S_{Pb}$ for coherent $J/\psi$ photoproduction in Pb-Pb UPCs predicted using Eq. (6) [11, 12], which is comparable to the experimental uncertainty of the LHC data for this process [4–6].

In the same formalism, we estimate the cross section of incoherent $J/\psi$ photoproduction on nuclear targets [18]:

$$\frac{\sigma^{\rm pQCD}_{\gamma A\to J/\psi A'}(W_{\gamma p})}{dt} = \frac{d\sigma_{\gamma p\to J/\psi p}(W_{\gamma p})}{dt}\int d^2\vec{b}\,T_A(b)\left[1-\frac{\sigma_2}{\sigma_3}\left(1-e^{-\frac{\sigma_3}{2}T_A(b)}\right)\right]^2. \tag{11}$$

For the $t$ dependence of the elementary $\gamma p \to J/\psi p$ cross section, we use the following simple exponential form:

$$\frac{d\sigma_{\gamma p\to J/\psi p}(W_{\gamma p})}{dt} = \frac{d\sigma_{\gamma p\to J/\psi p}(t=0)}{dt}e^{B_{J/\psi}t}, \tag{12}$$

where $B_{J/\psi}(W_{\gamma p}) = 4.5 + 0.4\ln(W_{\gamma p}/90\text{ GeV})$, which describes well the HERA data on the $t$ dependence of the cross section of $J/\psi$ photoproduction on the proton, see, e.g. [12].

## III. RESULTS AND DISCUSSION

Figure 1 shows our results for the $d\sigma_{\gamma A\to VA}(W_{\gamma p})/dt$ cross section for $\rho$ (top panel) and $J/\psi$ (lower panel) coherent photoproduction on $^{208}$Pb as a function of $|t|$. The cross sections are normalized to their values at $t = t_{\rm min}$, where $t_{\rm min} = -m_N^2 M_\rho^4/W_{\gamma p}^4$, and are evaluated at $W_{\gamma p} = 62$ GeV for $\rho$ and $W_{\gamma p} = 124$ GeV for $J/\psi$, which corresponds to $y = 0$ for Pb-Pb UPCs at $\sqrt{s_{NN}} = 5.02$ TeV. In the upper panel, the red solid curve labeled "mVMD-GGM" corresponds to Eq. (3). In the bottom panel, the red solid curve labeled "LTA" shows the result of Eq. (9) calculated with the lower value of $\sigma_3$, which corresponds to the upper limit on the shadowing effect for $J/\psi$ photoproduction. For reference, we also show the normalized nuclear form factor squared obtained using the nucleon density of $^{208}$Pb of Ref. [41] (the blue dot-dashed curve labeled "$|F_A(t)/A|^2$"). In the $\rho$ meson case, we also show the result of the calculation at $W_{\gamma p} = 10$ GeV corresponding to the RHIC kinematics (the green dashed line labeled "RHIC"). One can see that the normalized momentum transfer distribution is a weak function of $W_{\gamma p}$ between the RHIC and LHC energies.

One can see from the figure that nuclear shadowing modifies the $t$ dependence of $d\sigma_{\gamma A\to VA}(W_{\gamma p})/dt$ by shifting the positions of the diffractive minima and maxima towards smaller values of $|t|$. For instance, the shift of the first minimum is $\Delta p_t \approx 18$ MeV for $\rho$ and $\Delta p_t \approx 14$ MeV for $J/\psi$. Note that in the $\rho$ meson case, the predicted $t$ dependence very weakly depends on details of the model of cross section fluctuations. In the $J/\psi$ case, the effect of cross section fluctuations is implicit in Eq. (9) and the $\Delta p_t$ shift depends on the value of the average $\sigma_3$ cross section, which has a significant uncertainty and constrained to lie in the $\sigma_3 = 26-45$ mb interval. The result of the calculation with the lower value of $\sigma_3$, which corresponds to the scenario with the larger gluon shadowing in the leading twist model of nuclear shadowing [36], is presented in Fig. 1. For the larger value of $\sigma_3$ and the correspondingly smaller gluon shadowing, the modification of the $t$ distribution of $d\sigma_{\gamma A\to J/\psi A}(W_{\gamma p})/dt$ compared to $|F_A(t)/A|^2$ is smaller; the corresponding shift is $\Delta p_t \approx 6$ MeV.

The shift of the $t$ dependence of the $d\sigma_{\gamma A\to VA}(W_{\gamma p})/dt$ cross section shown in Fig. 1 can be interpreted as an increase (broadening) in the impact parameter space of the nucleon density in nuclei in the case of $\rho$ and the nuclear gluon distribution in the case of $J/\psi$. Characterizing the average transverse size of these distributions by the equivalent radius of $R_A$, one can estimate the relative increase of $R_A$ as $\Delta R_A/R_A \approx \Delta p_t/p_t$, which gives $\Delta R_A/R_A \approx 1.14$ for $\rho$ and $\Delta R_A/R_A \approx 1.05 - 1.11$ for $J/\psi$. The latter estimate agrees with the results of the analysis of the average transverse size of the nuclear gluon distribution of Ref. [36]. The transverse broadening of the nuclear gluon and sea quark distributions caused by nuclear shadowing can also be studied in other exclusive processes such as, e.g., deeply virtual Compton scattering, where it leads to dramatic oscillations of the beam-spin cross section asymmetry [36].

Figure 2 shows our predictions for $d\sigma_{AA\to\rho A'A}(y=0)/dydt$ as a function of $|t|$ (top panel) and $d\sigma_{AA\to\rho A'A}(y=0)/dydp_t$ as a function of $p_t$ (bottom panel) for Pb-Pb UPCs at $\sqrt{s_{NN}} = 5.02$ TeV for Run 2 at the LHC ($A'$ denotes

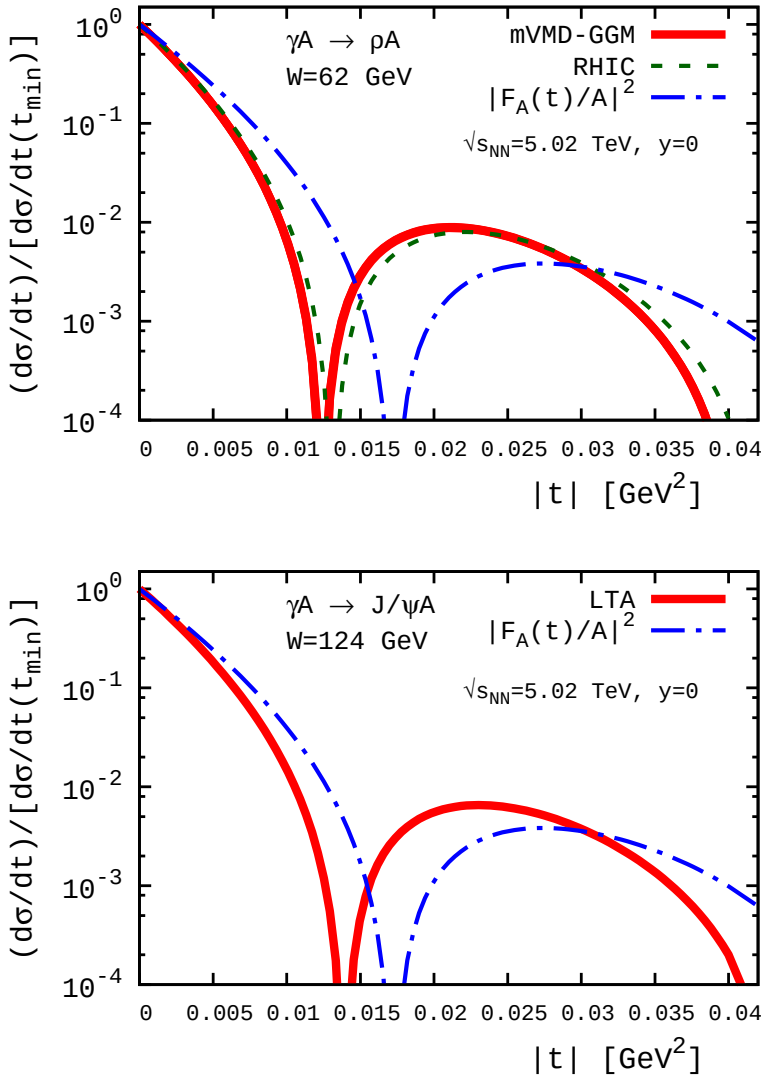


FIG. 1: The $d\sigma_{\gamma A\to VA}(W_{\gamma p})/dt$ cross section for $\rho$ (top panel) and $J/\psi$ (lower panel) for $^{208}$Pb normalized to its value at $t = t_{\rm min}$ as a function of $|t|$. The cross section are calculated at $W_{\gamma p} = 62$ GeV for $\rho$ and $W_{\gamma p} = 124$ GeV for $J/\psi$, corresponding to the LHC Run 2 $\sqrt{s_{NN}} = 5.02$ TeV and $y = 0$. The resulting $t$ dependence is compared to that given by the normalized nuclear form factor squared $|F_A(t)/A|^2$. For $\rho$ meson, we also show the result of the calculation at $W_{\gamma p} = 10$ GeV corresponding to the RHIC kinematics (the green dashed line labeled "RHIC").

both coherent $A' = A$ and incoherent $A' \neq A$ cases). The blue dot-dashed and black dotted curves give the coherent [Eqs. (1) and (3)] and incoherent [Eqs. (4)] contributions, respectively; the red solid curve is the sum of the coherent and incoherent terms. One can see from the figure that while the incoherent contribution partially fills in the first diffractive minimum in the $t$ dependence, the minimum still remains visible and its position as a function of $|t|$ or $p_t$ is unaffected.

The differential $d\sigma_{AA\to J/\psi A'A}(y = 0)/dydt$ cross section for $J/\psi$ photoproduction is shown in Fig. 3. The upper panel corresponds to the calculations with the higher leading twist gluon shadowing (smaller $\sigma_3$) [36] (as in Fig. 1): The blue dot-dashed and black dotted curves give separately the coherent and incoherent contributions, while the red solid curve is their sum. In the lower panel, we compare the sum of coherent and incoherent contributions calculated using the higher (the red solid curve) and lower (the blue dot-dashed curve) gluon nuclear shadowing. One can see from the lower panel of the figure that the higher gluon shadowing leads to a larger shift of the $t$ distribution. Also, as in the $\rho$ meson case, the incoherent contribution partially fills in the first diffractive minimum, which still remains visible.

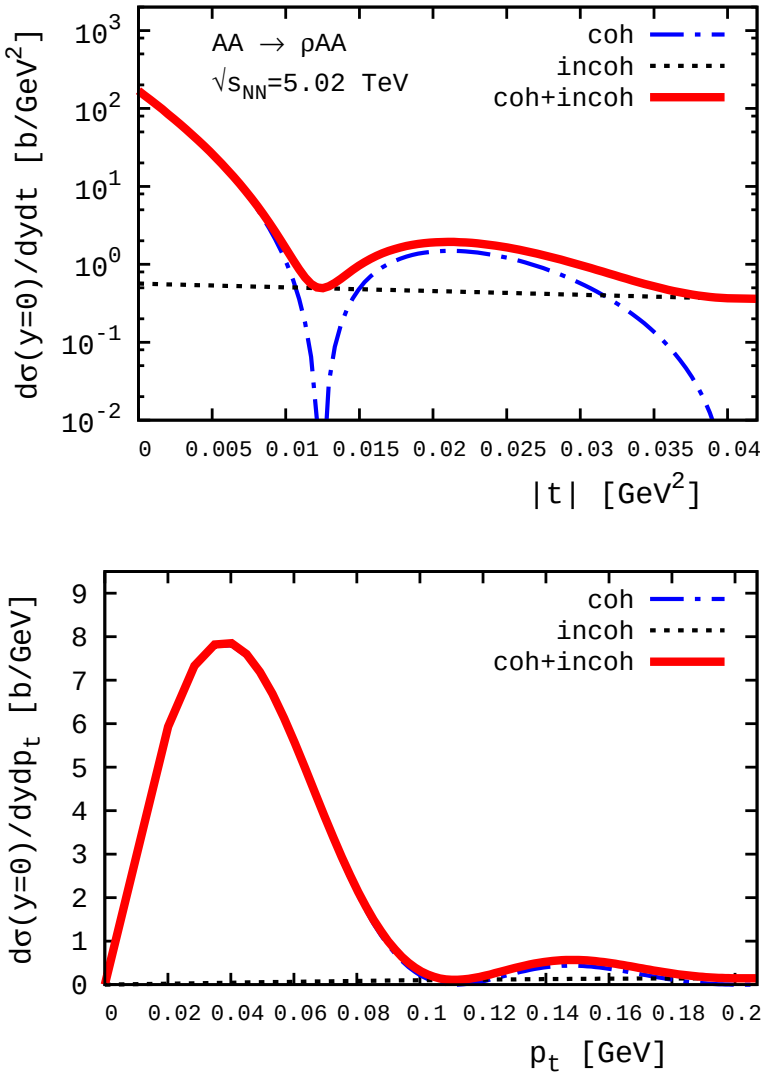


FIG. 2: Photoproduction of $\rho$ mesons in Pb-Pb UPCs at $y = 0$ and $\sqrt{s_{NN}} = 5.02$ TeV: $d\sigma_{AA\to\rho AA}(y = 0)/dydt$ as a function of $|t|$ (top panel) and $d\sigma_{AA\to\rho AA}(y = 0)/dydp_t$ as a function of $p_t$ (bottom panel). The blue dot-dashed and black dotted curves give separately the coherent and incoherent contributions, while the red solid curve is their sum.

Note that our results for the incoherent contribution to the $AA \to VA'A$ cross section were derived using completeness of final nuclear states and neglecting inelastic $\gamma N \to VX$ processes on the nucleon [18]. This approach underestimates the measured $t$-integrated cross section of incoherent $J/\psi$ photoproduction in Pb-Pb UPCs at the LHC at $\sqrt{s_{NN}} = 2.76$ TeV [4] by approximately a factor of 1.5. Hence, a more accurate treatment of the incoherent contribution will somewhat increase its magnitude at the values of $t$ shown in Fig. 3, which will result in a less pronounced first diffractive minimum.

The standard method of separating the coherent and incoherent contributions is an examination of their $t$ ($p_t$) dependence; this is illustrated in Figs. 2 and 3. In addition, one can experimentally suppress the incoherent contribution by using zero degree calorimeters registering forward neutrons. Since quasi-elastic scattering leads to emission of one or more neutrons with 85% probability, requiring that no neutrons are emitted (the so-called 0n0n-channel) suppresses the incoherent contribution at the 15% level, see the discussion in Ref. [18].

To further illustrate the effect of impact parameter dependent nuclear shadowing on the cross section of coherent $J/\psi$ photoproduction on nuclei, in Fig. 4 we show our results for the $J/\psi$ rapidity distribution in Pb-Pb UPCs at $\sqrt{s_{NN}} = 5.02$ TeV: the lower band labeled "b-dep." is calculated using Eq. (9), while the upper band labeled "b-indep." is calculated using Eq. (6). One can see from the figure that taking into account the non-trivial impact

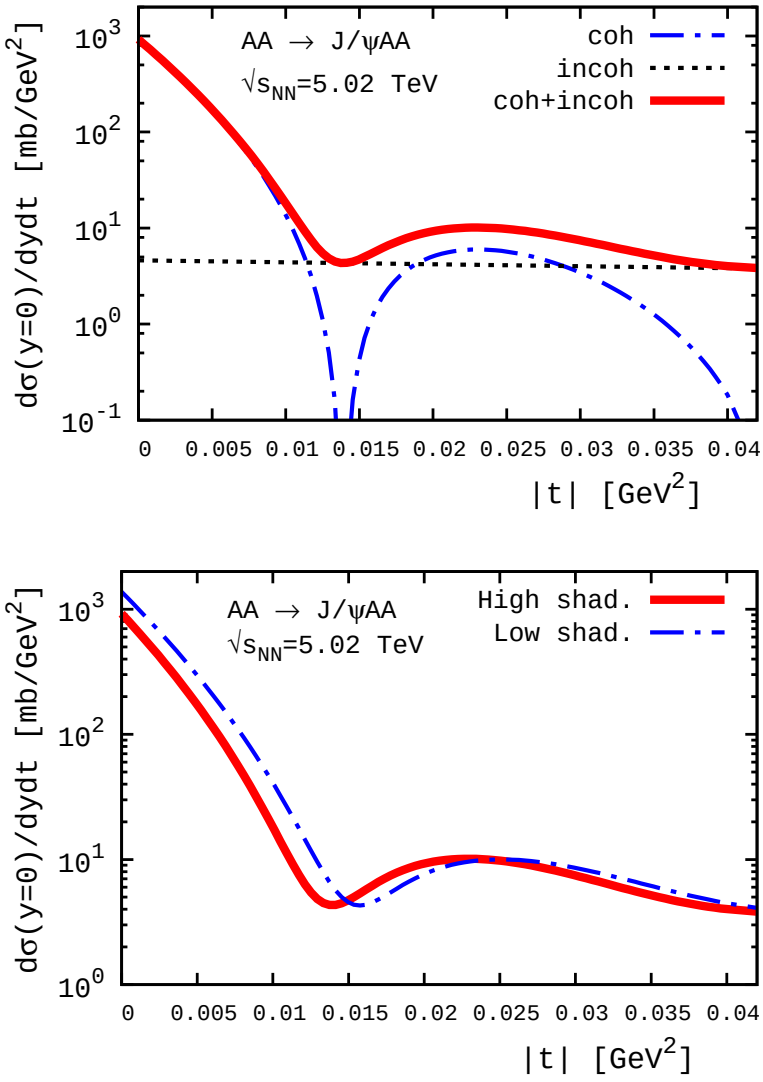


FIG. 3: Photoproduction of $J/\psi$ mesons in Pb-Pb UPCs at $y = 0$ and $\sqrt{s_{NN}} = 5.02$ TeV: $d\sigma_{AA\to J/\psi AA}(y = 0)/dydt$ as a function of $|t|$. Top panel: The blue dot-dashed and black dotted curves give separately the coherent and incoherent contributions calculated using the higher gluon shadowing, while the red solid curve is their sum. Bottom panel: The sum of coherent and incoherent contributions calculated using the higher (red solid curve) and lower (blue dot-dashed curve) gluon nuclear shadowing.

parameter dependence of $g_A(x, b, \mu^2)$ somewhat lowers our predictions for $d\sigma_{AA\to J/\psi AA}(y)/dy$. For instance, at $y = 0$, we predict that $d\sigma(y = 0)/dy = 2.82 - 3.93$ mb for the calculation with the impact parameter dependent shadowing (the "b-dep." curves) and $d\sigma(y = 0)/dy = 3.28 - 4.24$ mb for the "b-indep." case. It corresponds to a 15% reduction of $d\sigma(y = 0)/dy$ for the higher gluon shadowing scenario (the lower boundary of the shaded bands in Fig. 4) and 8% reduction of $d\sigma(y = 0)/dy$ in the lower gluon shadowing case (the upper boundary of the bands in Fig. 4). As we already mentioned in Sect. II, this effect does not affect the good agreement between our earlier predictions [11, 12] and the Run 1 LHC data [4–6].

As we mentioned in the Introduction, UPC measurements at the LHC compliment the physics program of a future Electron-Ion Collider. To illustrate the EIC potential for transverse imaging in real photon–nucleus scattering, in Fig. 5 we show the shift of the first diffractive minimum of the $d\sigma_{\gamma A\to J/\psi A}/dt$ (red solid curve) and $d\sigma_{\gamma A\to \rho A}/dt$ (blue dot-dashed curve) cross sections with the respect to the first minimum of $F_A^2(t)$, $\Delta p_t$, as a function of the atomic number of $A$ at $W_{\gamma p} = 45$ GeV. This value of $W_{\gamma p}$ conforms with the EIC kinematics and, in the case of $J/\psi$, corresponds to $x = M_{J/\psi}^2/W_{\gamma p}^2 = 0.005$. One can see from the figure that the $\Delta p_t$ shift is sizable and increases with

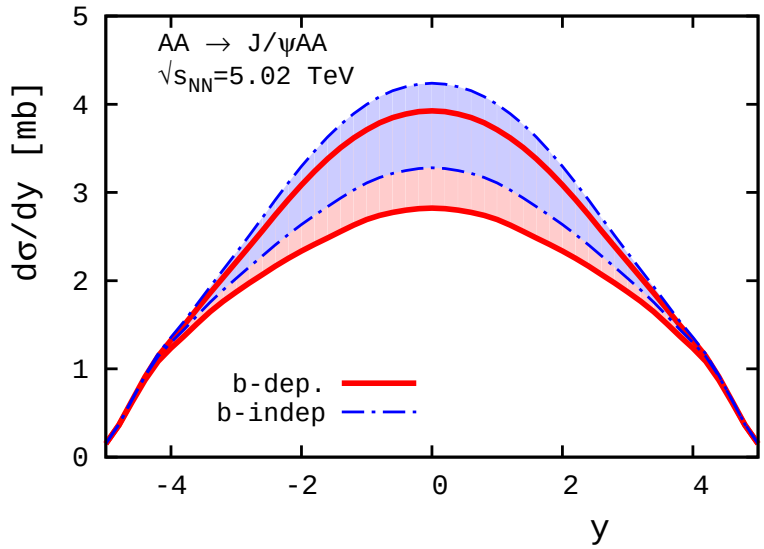


FIG. 4: The $J/\psi$ rapidity distribution in Pb-Pb UPCs at $\sqrt{s_{NN}} = 5.02$ TeV: the lower band labeled 'b-dep." corresponds to impact parameter dependent nuclear shadowing [Eq. (9)], while the upper band labeled "b-indep." is obtained using Eq. (6) neglecting the non-trivial impact parameter dependence of gluon nuclear shadowing.

a decrease of $A$. The latter is a consequence of the fact that while the position of the first minimum of $F_A^2(t)$ scales as $A^{-1/3}$, the position of the first minimum of $d\sigma_{\gamma A\to VA}/dt$ scales somewhat slower due to nuclear shadowing, which makes $\Delta p_t$ a decreasing function of $A$. Note that this $A$-behavior of $\Delta p_t$ changes for small $A \leq 4$, where one should approach the formal limit of $\Delta p_t \to 0$ for $A \to 1$. At the same time, $\Delta p_t/p_t$ behaves monotonously and increases with an increase of $A$ for all atomic numbers.

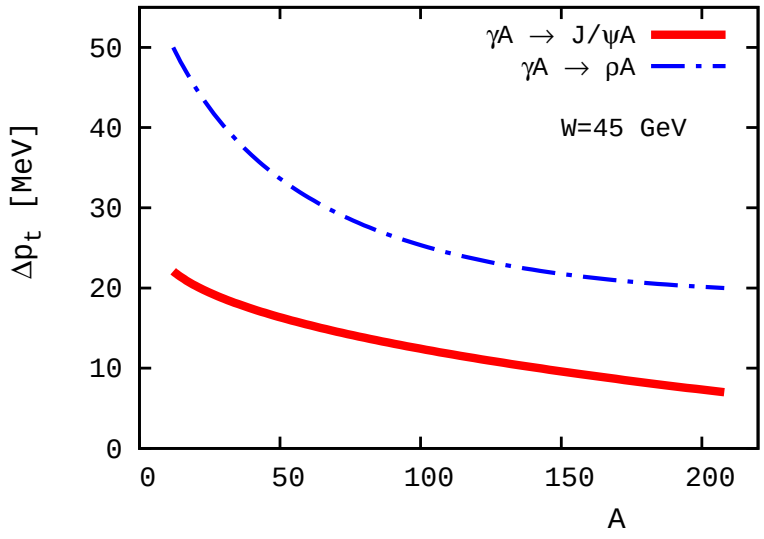


FIG. 5: The shift of the first diffractive minimum of $d\sigma_{\gamma A\to J/\psi A}/dt$ (red solid curve) and $d\sigma_{\gamma A\to \rho A}/dt$ (blue dot-dashed curve) with the respect to that of $F_A^2(t)$, $\Delta p_t$, as a function of the atomic number $A$ at $W_{\gamma p} = 45$ GeV. In the $J/\psi$ case, it corresponds to $x = M_{J/\psi}^2/W_{\gamma p}^2 = 0.005$.

In our analysis, we neglected the interference contribution in Eq. (1) and the resulting photon contribution to the transverse momentum distributions [42]. This contribution is confined to very low $p_t < 10$ MeV and, hence, does not affect the results of our analysis focusing on the first diffractive minimum situated at much larger values of $p_t$.

Note that the shift of the diffractive minima due to nuclear shadowing that we observe is caused by soft diffraction in the case of $\rho$ and by leading twist hard diffraction in the case of $J/\psi$. In the $J/\psi$ case, this mechanism can be contrasted with predictions of other approaches available in the literature. In the $k_t$-factorization approach [43], the unintegrated nuclear gluon distribution receives contributions from multiple scattering of both quark–antiquark (so-called Glauber regime) and quark–antiquark–gluon dipoles on a nucleus, which determine the initial condition for the nonlinear evolution equation. Note that the successful description of the proton diffractive structure functions measured in $ep$ DIS at HERA requires both quark-antiquark and quark-antiquark–gluon dipoles in the color dipole formalism; it provides a connection to our leading twist approach, where the nuclear gluon shadowing is determined by the gluon diffractive parton distribution of the proton. The inclusion of the quark–antiquark–gluon contribution leads to a noticeable suppression of the predicted impact parameter distribution of coherent $J/\psi$ photoproduction on Pb with an increase of the photon energy. In the momentum space, it should correspond to a shift of the $t$ distribution toward smaller $|t|$, cf. Ref. [36]. Thus, regardless of the dynamical mechanism of nuclear shadowing, large nuclear gluon shadowing leads to the modification of the $t$ distribution of $J/\psi$ photoproduction in ion UPCs. At the same time, in the implementations of the color dipole framework, where coherent photoproduction of $J/\psi$ on nuclei proceeds via multiple rescattering of quark–antiquark dipoles [13, 44, 45], the shadowing correction is not large since the average dipole–nucleon cross section is determined by the small size of $J/\psi$. As a result, the modification of the $t$ distribution of $J/\psi$ photoproduction on nuclei compared to $F_A^2(t)$ is smaller than predicted in our analysis.

## IV. CONCLUSIONS

In this paper, using the theoretical approaches describing well the available data on $t$-integrated coherent photoproduction of light and heavy vector mesons in Pb-Pb UPCs at the LHC during Run 1, we calculated the momentum transfer distributions for this process for $\rho$ and $J/\psi$ vector mesons in the kinematics of Run 2 at the LHC. We demonstrated that nuclear shadowing not only suppresses the absolute value of the cross sections, but also shifts the momentum transfer distributions toward smaller values of the momentum transfer $|t|$. This result can be interpreted as a broadening in the impact parameter space of the effective nucleon density in nuclei in the case of $\rho$ and the nuclear gluon distribution in the case of $J/\psi$. Characterizing the average transverse size of these distributions by the equivalent radius of $R_A$, for the relative increase of $R_A$ we found $\Delta R_A/R_A \approx 1.14$ for $\rho$ and $\Delta R_A/R_A \approx 1.05 - 1.11$ for $J/\psi$.

The observed broadening of the transverse distributions is a model-independent consequence of nuclear shadowing, whose suppression effect at small impact parameters is stronger than at the nucleus periphery. The transverse broadening of the nuclear gluon and sea quark distributions caused by nuclear shadowing can also be studied at EIC in such hard exclusive processes as, e.g., deeply virtual Compton scattering, where it leads to dramatic oscillations of the beam-spin cross section asymmetry. All such measurements at the LHC and EIC will for the first time measure the impact parameter dependent quark and gluon distributions in nuclei and, hence, make an important step in obtaining a three-dimensional image of parton distributions.

### Acknowledgments

M.S.'s research was supported by the US Department of Energy Office of Science, Office of Nuclear Physics under Award No. DE-FG02-93ER40771. V.G. would like to thank Pennsylvania State University for hospitality during the final stage of this work. M.Zh.'s research was supported in part by RF Ministry of Science and Education under contract No. 14.610.21.0003.

[1] A. Accardi *et al.*, Eur. Phys. J. A **52**, no. 9, 268 (2016).
[2] A. J. Baltz *et al.*, Phys. Rept. **458**, 1 (2008).
[3] J. Adam *et al.* [ALICE Collaboration], JHEP **1509**, 095 (2015).
[4] E. Abbas *et al.* [ALICE Collaboration], Eur. Phys. J. C **73**, no. 11, 2617 (2013).
[5] B. Abelev *et al.* [ALICE Collaboration], Phys. Lett. B **718**, 1273 (2013).
[6] V. Khachatryan *et al.* [CMS Collaboration], [arXiv:1605.06966 [nucl-ex]].
[7] V. Rebyakova, M. Strikman and M. Zhalov, Phys. Lett. B **710**, 647 (2012).
[8] L. Frankfurt, V. Guzey, M. Strikman and M. Zhalov, Phys. Lett. B **752**, 51 (2016).
[9] G. Sampaio dos Santos and M. V. T. Machado, Phys. Rev. C **91**, no. 2, 025203 (2015).
[10] A. Adeluyi and C. A. Bertulani, Phys. Rev. C **85**, 044904 (2012).

[11] V. Guzey, E. Kryshen, M. Strikman and M. Zhalov, Phys. Lett. B **726**, 290 (2013).
[12] V. Guzey and M. Zhalov, JHEP **1310**, 207 (2013).
[13] T. Lappi and H. Mantysaari, Phys. Rev. C **87**, no. 3, 032201 (2013).
[14] V. P. Goncalves, B. D. Moreira and F. S. Navarra, Phys. Rev. C **90**, no. 1, 015203 (2014).
[15] R. Debbe [STAR Collaboration], J. Phys. Conf. Ser. **389**, 012042 (2012).
[16] S. R. Klein [STAR Collaboration], PoS DIS **2016**, 188 (2016).
[17] A. Takahara [PHENIX Collaboration], doi:10.3204/DESY-PROC-2012-02/114;
A. Takahara, "$J/\psi$ photoproduction in Au+Au ultra-peripheral collisions at $\sqrt{S_{NN}}$ = 200 GeV at RHIC," Ph.D. thesis (2013).
[18] V. Guzey, M. Strikman and M. Zhalov, Eur. Phys. J. C **74**, no. 7, 2942 (2014).
[19] V. Guzey, E. Kryshen and M. Zhalov, Phys. Rev. C **93**, no. 5, 055206 (2016).
[20] T. H. Bauer, R. D. Spital, D. R. Yennie and F. M. Pipkin, Rev. Mod. Phys. **50**, 261 (1978) Erratum: [Rev. Mod. Phys. **51**, 407 (1979)].
[21] L. Frankfurt, M. Strikman and M. Zhalov, Phys. Lett. B **537**, 51 (2002).
[22] L. Frankfurt, M. Strikman and M. Zhalov, Phys. Rev. C **67**, 034901 (2003).
[23] G. Agakishiev *et al.* [STAR Collaboration], Phys. Rev. C **85**, 014910 (2012).
[24] C. Adler *et al.* [STAR Collaboration], Phys. Rev. Lett. **89**, 272302 (2002).
[25] M. L. Good and W. D. Walker, Phys. Rev. **120**, 1857 (1960).
[26] B. Blaettel, G. Baym, L. L. Frankfurt, H. Heiselberg and M. Strikman, Phys. Rev. D **47**, 2761 (1993).
[27] B. I. Abelev *et al.* [STAR Collaboration], Phys. Rev. C **77**, 034910 (2008).
[28] S. Aid *et al.* [H1 Collaboration], Nucl. Phys. B **463**, 3 (1996).
[29] J. Breitweg *et al.* [ZEUS Collaboration], Eur. Phys. J. C **2**, 247 (1998).
[30] M. G. Ryskin, Z. Phys. C **57**, 89 (1993).
[31] S. J. Brodsky, L. Frankfurt, J. F. Gunion, A. H. Mueller and M. Strikman, Phys. Rev. D **50**, 3134 (1994).
[32] A. G. Shuvaev, K. J. Golec-Biernat, A. D. Martin and M. G. Ryskin, Phys. Rev. D **60**, 014015 (1999).
[33] M. G. Ryskin, R. G. Roberts, A. D. Martin and E. M. Levin, Z. Phys. C **76**, 231 (1997).
[34] L. Frankfurt, W. Koepf and M. Strikman, Phys. Rev. D **57**, 512 (1998).
[35] M. Burkardt, Phys. Rev. D **62**, 071503 (2000) Erratum: [Phys. Rev. D **66**, 119903 (2002)].
[36] L. Frankfurt, V. Guzey and M. Strikman, Phys. Rept. **512**, 255 (2012).
[37] I. Helenius, K. J. Eskola, H. Honkanen and C. A. Salgado, JHEP **1207**, 073 (2012).
[38] A. Aktas *et al.* [H1 Collaboration], Eur. Phys. J. C **48**, 749 (2006).
[39] A. Aktas *et al.* [H1 Collaboration], Eur. Phys. J. C **48**, 715 (2006).
[40] J. Pumplin, D. R. Stump, J. Huston, H. L. Lai, P. M. Nadolsky and W. K. Tung, JHEP **0207**, 012 (2002).
[41] H. De Vries, C. W. De Jager and C. De Vries, Atom. Data Nucl. Data Tabl. **36**, 495 (1987).
[42] S. R. Klein and J. Nystrand, Phys. Rev. Lett. **84**, 2330 (2000).
[43] A. Cisek, W. Schafer and A. Szczurek, Phys. Rev. C **86**, 014905 (2012).
[44] A. Caldwell and H. Kowalski, arXiv:0909.1254 [hep-ph].
[45] T. Toll and T. Ullrich, Phys. Rev. C **87**, no. 2, 024913 (2013).